UDC 621.37

KA-BAND GROUND-BASED NOISE SAR TRIALS IN VARIOUS CONDITIONS

K.A. LUKIN, A. G. STOVE, K. KULPA, D. CALUGI, V.P. PALAMARCHUK, P.L. VYPLAVIN

Interest to noise radars is growing because they provide good electromagnetic compatibility, the best Low Probability of Interception (LPI) and Probability of Exploiting (LPE) characteristics and other desirable features whilst current progress in electronics makes them more and more affordable. One of the noise radar applications is SAR imaging. Correct operation of SAR requires high stability of radar parameters including the parameters of the probing signal. This paper is devoted to experimental investigation of Ka-band ground based noise SAR and estimation of noise level, dynamic range, range resolution, residual fluctuations and sidelobe levels. In the paper, we briefly describe design of the Noise Waveform SAR and present the trials results.

Keywords: noise radar, SAR, interferometry.

I. INTRODUCTION

Currently, noise radars (NR) is gaining more interest from engineers and researchers. Progress in analog and digital electronics enables their design to be simpler and cheaper and, thus, increases NR affordability. Noise signals provide high robustness to interference, good electromagnetic compatibility, low probability of interception (LPI), simple generation of signals with low range sidelobes and having a highly stable frequency spectrum shape. The presence of so called residual fluctuations in range profiles is a well known effect of using noise signals. They appear in the compressed signals as random fluctuations of the cross-correlation function related to the randomness of sounding signal. Their level is dependent on time-bandwidth product of the signal. Proper choice of the integration time and the signal bandwidth enables the negative effects of residual fluctuations to be reduced to a level where they have only a minor effect on the dynamic range of the radar[1-3].

In the Laboratory of Nonlinear Dynamics of Electronic Systems of IRE NASU a Ka-band Ground Based noise waveform Synthetic Aperture Radar (GB NW-SAR) has been designed for imaging of illuminated areas and detection of small structural changes in buildings, constructions or environmental formations using differential SAR interferometry technique [4,5]. The SAR principle in this radar is realized using a novel design of Antennas with Beam Synthesis (ABS) [6-8]. Two such antennas can be used in this system providing operation in bistatic and monostatic regimes. A truly random Ka-band signal with bandwidth up to 480 MHz provides high range resolution of the SAR images. A series of experiments with the aimof testing this SAR system have been carried out against various backgrounds such as: on asphalt and ground areas with low incidence angles and on the water surface of a wide pond.

In the paper, we shortly describe main performance of the Noise Waveform SAR, the trials results, and discuss its future applications.

2. KA-BAND GROUND BASED NOISE WAVEFORM SAR

The GB NW-SAR operates at (36.0 – 36.5) GHz. To obtain good angular resolution and coverage without turning the whole system, scanning is achieved by moving a single slot along the desired antenna aperture and forming the angular resolution by the equivalent of focused synthetic aperture processing [6-8]. Physically, the scanner is a length of waveguide with its broad wall removed and a piece of copper sheet containing the resonant radiating/receiving slot and some matching structures is pulled along its front face. The elevation pattern is formed with a 2D horn structure [6-8]. The GB NW-SAR is shown in fig. 1.

Fig. 1. The Ka-band noise SAR photo

The system can either be used as a short-baseline bistatic system with identical transmit and receive antennas, or monostatically with a small horn transmit antenna directly above the receive antenna which is used to form the narrow synthesized beam [6-8]. This synthetic aperture mode of operation gives the advantage that the SAR imagery provides an indication of the close-to-carrier noise, but it did mean that any movement of a target during the 20 seconds or so which it took to form an image led to its being defocused in azimuth. The farther unit is the receiver; the vertical green waveguide feed to the monostatic transmit transmitter can be seem attached to this unit. The nearer unit is the transmitter. The box with the heat sink is the control unit with the power supply. The copper band with the radiating slot in it can be seen at the near end of the transmitter. It is designed to fit standard 35mm film sprockets. The unit below the baseplate contains the stepper motor which drives the. The scan is indexed by an optical sensor on the back on the copper tape but the system also uses an absolute-position shaft encoder above which can be seen above the motor unit. The main performance of the system is summarized in Table 1.

Table 1

Main performance of Ka-band Noise Waveform SAR

Operational mode	Bistatic
Waveform	CW Noise
Working frequencies, GHz	36-37
Power Spectrum Bandwidth at -3 dB level, GHz	0.45
Antenna pattern width in elevation, deg	20
Antenna pattern width in azimuth, deg	80
Maximal transmitted power, W	0.15
Nominal Power spectrum shape	"Gaussian" or "Rectangular"
Receiver frequency response width, GHz	0.5 or 1.0
Receiver Noise Figure, dB	< 7
ADC Sampling rate, GSamples/sec	1.0 or 2.0
Synthetic aperture length, m	0.7
Cross-range resolution at 50 m distance, m	0.3
Range resolution, m	0.35
Precision of displacement detection, mm	0.03
Single scan duration, s	≈ 22

3. EXPERIMENTAL INVESTIGATIONS

The trials were planned to concentrate on proving the resolution, dynamic range and stability of the radar. The noise limited sensitivity was estimated based on the return from a corner reflector. Other trial aims were to measure returns from water, which led to the SAR image of the lake being obtained. This trial provided an illustration of the capabilities of the GB NW-SAR and a comparison with some of the more tightly-controlled trials. In all, a comprehensive set of tests were able to be carried out during the week of the trials.

The antenna took up 237 discrete positions during the scan. At each of the antenna positions signals were transmitted, received and recorded at 1GHz rate. Thus, each data set consists of 237 subsets of data. Each data subset consists of 1 940 480 samples, representing just under 1.95ms of data. The data was recorded for every half wavelength of the movement of the real aperture along the line of the synthetic aperture. The first step in the analysis was to correlate the signal with the reference for each data set. For the 'lake' data set the correlation was performed out to 10000 range cells (1500m at 1GHz sample rate) but nothing was seen beyond about 4350 cells (about 650m). Correlation estimation yielded only real data, since both inputs to the correlation were real. Further processing requires analytic signals with complex values. The imaginary part for these signals may be obtained using a Hilbert transform.

Two algorithms were used for obtaining angular resolution. First images were generated using simple FFT-based approach. The successive samples at each range cell were stacked together, zero-filled to 256 points and Fourier transformed to give the angular resolution. This is in fact a beam-forming rather than a SAR process. The data was given a cosine-squared weighting to control the azimuth sidelobes. The angular resolution of the data was 0.24°, determined by the synthetic aperture length. The azimuth cell width was slightly less, 0.22°, determined by the FFT size.

At this stage, the image of the lake was examined, to get a 'feel' of the performance of the radar in a relatively simple scene, i.e. one which was known to have a relatively 'clear' area (the lake itself) at short range. Fig. 2 is a SAR image of the lake, fig. 3 is a 'Google Earth' picture of the area

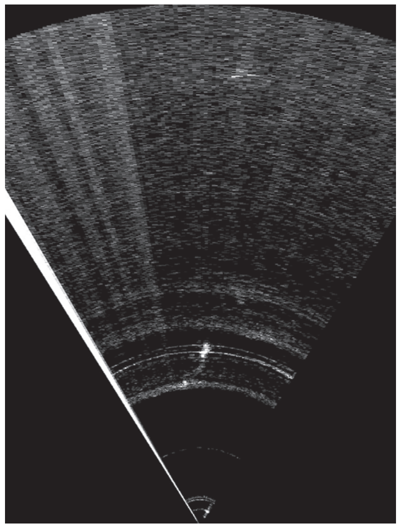

Fig. 2. SAR image of the Lake

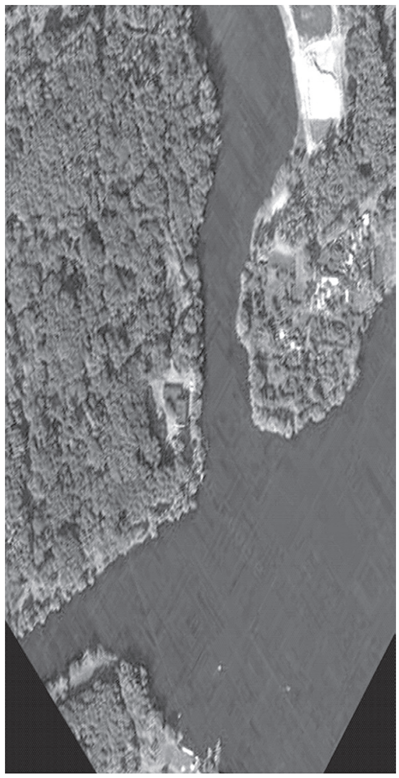

Fig. 3. Satellite image of the Lake

The arcs in the SAR image are caused by failure of the target to focus perfectly in bearing, because part of it has decorrelated (i.e., moved) during the relatively long time taken for the antenna to travel across the synthetic aperture.

The prominent white line at the upper edge of the limit is due to the d.c. offsets in the signal and reference, which, having no bandwidth, produces a return at all ranges, but, being always present, focuses up at broadside (the 'end' of the image around which the SAR image 'folds'). It can be removed by calculating the mean value of each data set and subtracting this value from each element before performing the correlations. Since the mean value of any finite number of normally-distributed random values will not be exactly zero, this process introduces a small bias into the data, equivalent to a high-pass filtering of the data. In practice, the noise bandwidth would not go exactly down to zero, so this is not an issue.

Fig. 4 shows an example of a SAR image of the same area obtained with removal of DC offset and using a straightforward SAR imaging algorithm rather than FFT-based one. This algorithm requires more processing time but takes into account detailed information about movement of the antenna's phase centers and gives results with higher precision. Main features of the scenario are marked in the image. The most distant target is at a range of about 640m, which is believed to have been a record for a noise waveform radar at the time when the trials were done. The brightness is scaled using a range-squared 'sensitivity time control' on the image to avoid the barge dominating the dynamic range and have then increased the contrast to help detection.

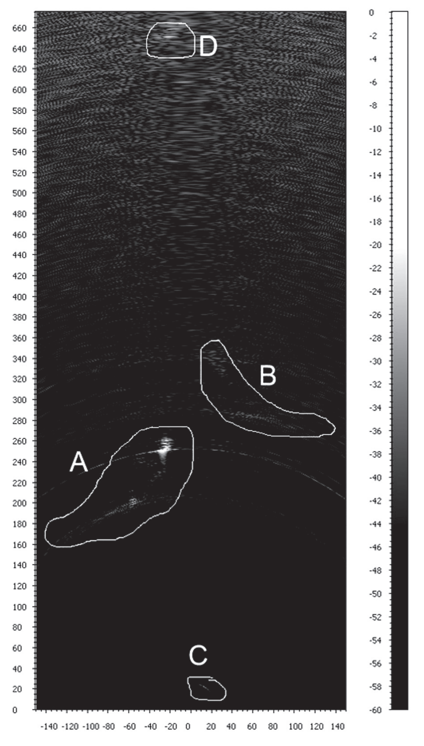

Fig. 4. SAR image of the Lake with main features marked: A) Lake shore and the little building; B) Shore of the island; C) Barge very close to position of radar; D) Obvious distant target

It can be seen that the signal/background on the target in the middle of the SAR image is between 50 dB and 60 dB. The dynamic range against some of the targets at short range exceeds 60 dB. The general level of the azimuth sidelobes is about 40 dB, which is good for a one-way antenna pattern. Another image was also obtained in another direction at the same site, one which contained more targets. This is the scene at the boat club which is shown in fig. 5. Fig. 6 shows its SAR image. SAR images generated from this area enable clear detection of such objects as fence, car (labeled 'auto'), trees, and corner reflectors (labeled 'scatteratori'). Fig. 7 shows SAR image of two corner reflectors spaced by 1 m and placed in the walking path (fig. 5) at the distance of 31 m from the GB NW-SAR.

Fig. 5. Photo of the measurements area

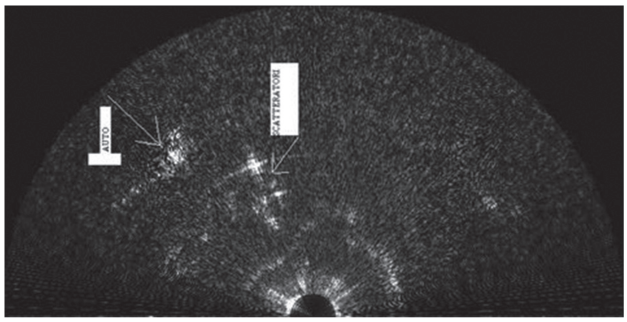

Fig. 6. SAR image generated from the area shown in fig 5

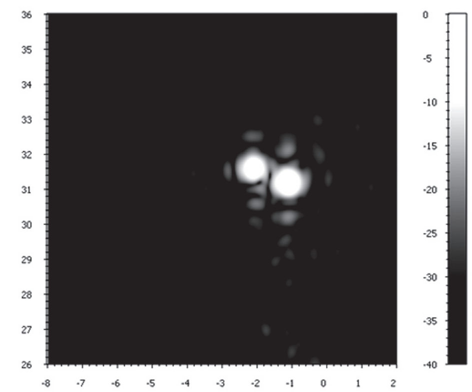

Fig. 7. Zoomed in image of two corner reflectors at area shown in Fig.5. Distance between the reflectors is 1m

This image clearly shows that the radar is capable of achieving its expected resolution of about 50 cm in both down-and cross-range.

3.1. Image of the Asphalted Court

A series of SAR images of an area covered by asphalt were obtained at low grazing angles. Figure 8 shows the scene of measurements and figure 9 shows the SAR image obtained in a straightforward manner and adds labels to indicate some of the features which can be seen in this image. This image extends out to a maximum range of 100m.

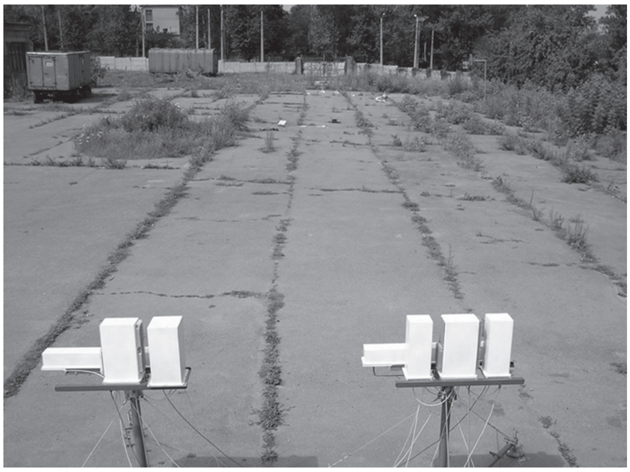

Fig. 8. Asphalted court and GB NW-SAR in bistatic configuration

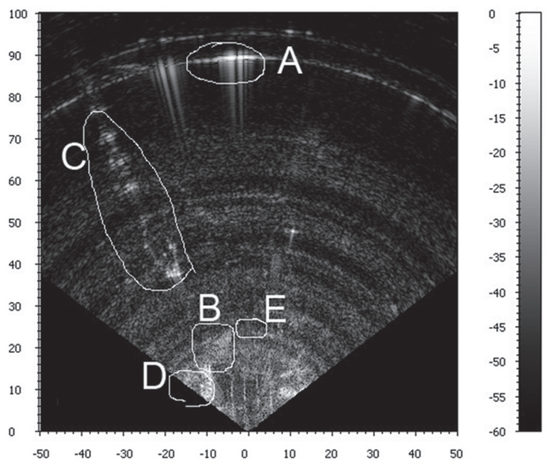

Fig. 9. SAR image of asphalted court with main features of the scene marked: A) gate at the end of the area; B) region of vegetation seen on the left of the photograph; C) building at the edge of the area; D) some vehicles at the left side of the radar; E) the region containing the corner reflectors

A significant feature of this image is that the noise floor is similar to that of the SAR image of the lake, and so is the dynamic range of the image.

3.2. Indoor measurements

In order to characterize operation of the GB-NW SAR on an indoor scenario measurements have been performed during NRT 2012 conference in Yalta Crimea. The experiments were done inside a conference hall with concrete walls and some chairs on the floor. A SAR image was obtained with the best specialist in noise radar sitting on the chairs in front of the noise GB NW SAR. Figure 10 shows photograph of the scene and the obtained SAR image of the room with people and with empty chairs. The measurement was perfectly safe because radiated power was as low as 1 mW. It can be seen that the room, radar community and empty chairs are well resolved and clearly seen in the obtained SAR images. The strongest reflection in the image corresponds to the mirror reflection from the far wall in front of the radar.

Fig. 10. Photograph of the indoor scenario

4. SENSITIVITY

The power budget of the radar at maximum sensitivity when using synthetic-aperture antennas on both transmit and receive was estimated theoretically using the known specifications of the radar system and taking into account the integration time. The integration is performed in the signal processing by performing range compression and synthetic aperture processing.

For the tests in the asphalted court, the signal to noise ratio expected for the largest corner reflector (a tridehral 30cm long on the sides) was 97.5dB. The measured signal to noise ratio was 39dB.

The results for all four corner reflectors are summarized below

Table 2

Expected Sensitivities

Side	Expected SNR	Observed SNR	Discrepancy
30 cm	97.5dB	39dB	58.5dB
15 cm	85.5dB	42dB	43.5dB
		51dB	34.5dB
10 cm	78.4dB	45dB	33.4dB

If we assume that any uncontrolled factors will only reduce the signal to noise ratio, and noting that the latter two rows of the table both show discrepancies of about 34dB, we may conclude that the sensitivity of the radar is about 30dB less than simple theory would suggest.

One cross-check is to use the assumption that the transmit-receive isolation is of the order of -100dB, so the leakage power for 7dBm transmit power would be -92dBm. In contrast, the power returned from the smallest corner reflector would be expected to be -71.5dBm, i.e. about 20dB above the leakage signal. The measured ratio is +25dB. This suggests that the signal levels are as expected, implying that the source of the discrepancy in the signal to noise ratios would be

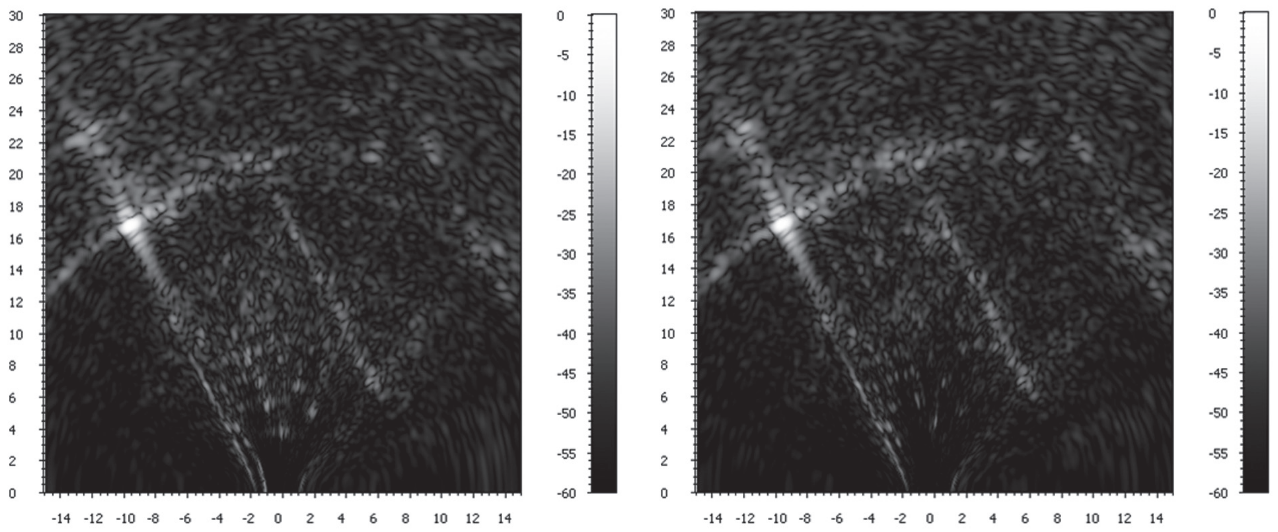

a) b)

Fig. 11. SAR images of scenario shown in fig.10 obtained (a) with people on the chairs and (b) without them

expected to be found in the background noise levels. The most likely explanation of this mismatch is that the measurements at the asphalted court were done during windy conditions and vegetation around the radar was moving during the scanning. This led to losing of coherence of its responses in the SAR image and spreading out in azimuth. This is proven by the noisy arcs visible in the image at the ranges corresponding to the areas with highest vegetation amounts.

The sensitivity may also be limited by the far-out sidelobes of the targets.

5. RANGE AND DOPPLER RESOLUTION

Fig. 12 shows the down-range cut through the return from the largest corner reflector

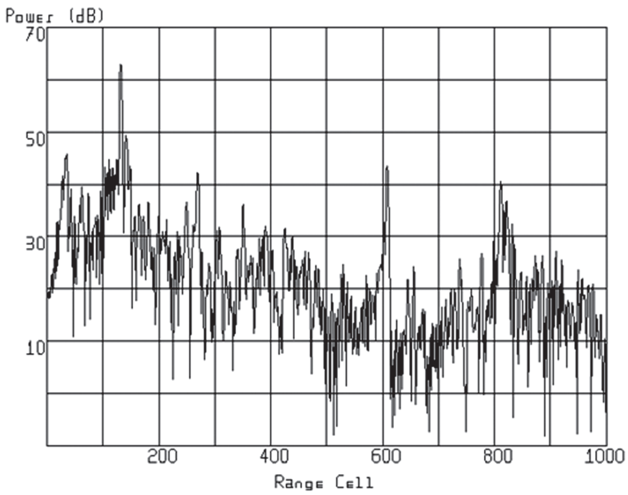

Fig. 12. Range cut through 30cm corner reflector

The corner reflector is at range cell 131. It is clear that other targets at longer range limit the ability to see the noise floor. It can be seen, however, that the dynamic range is at least 60dB and so the far-out sidelobe level must be below -60dB. Fig. 13 shows the cut 'zoomed in' around the target.

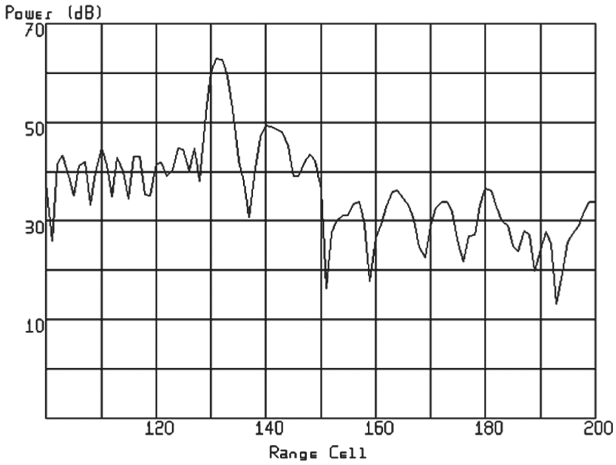

Fig. 13. Range cut near the corner reflector

This shows that the down-range sidelobes are probably at least 30dB below the peak. However, the second peak around cell 140, 13dB below the peak, is probably part of the same return. The difference in range between them is about 1.35m which is compatible with the physical size of the radar equipment, so this return may be due to internal reflections within the radar. The signal in cell 149 may also be due to another internal reflection, but this is more speculative. It might be a separate return, but the range extent of all the targets on the SAR image suggests that it is present on all the targets. The range sidelobes could probably be improved by weighting the spectrum of the received signal. The 3dB width of the signal is about 3 cells (0.45m) which is compatible with the signal bandwidth of about 400MHz. Figure 14 shows the cut of the data from the corner reflector in the bearing domain.

In this image the corner reflector is in cell -100. The dynamic range is limited by instability in the return from the bushes, around cells 50 and 60. Examination of the return from the gate in figure 12, however, suggests that the cross-range dynamic range is also limited to about this level.

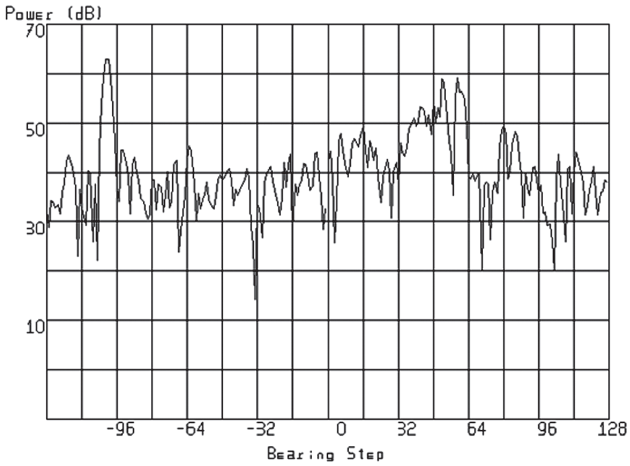

Fig. 14. Cross-range profile of the corner reflector

6. CONCLUSION

The Ka-band GB NW-SAR is capable of producing high resolution imagery, with close-to-ideal resolution and a demonstrated dynamic range of at least 60dB. It is capable of seeing navigational features at ranges out to about 650m. The experiment showed certain mismatch between the theoretical and measured signal-to-noise ratio which may be explained by losing of radar returns coherence due to objects randomly moving during measurement and by the bistatic angles being too high for correct operation of corner reflectors. It is therefore important to investigate signal-to-noise ratio by further experiments, may be to reveal other sources of the above mismatching between theory and the experiments.

The far-out sidelobes in range are at least 60dB below the peak, but in Doppler they are probably only 30dB down. This may happen due to instabilities of the scene and radar during the measurements on windy day. Apart from the features described above, the remaining sidelobe pattern appeared to be roughly elliptical in the range-Doppler.

ACKNOWLEDGEMENT

The authors are very much thankful to LNDES staff for carrying out the trial campaign in Kharkov.

References

[1] K.A.Lukin, “Noise Radar Technology”, Radiophysics and Electronics, Kharkiv, Institute for Radiophysics and Electronics NASU, 1999, vol.4, #. 3, pp.105-111. *Translated to English*: Lukin, K.A. *Noise Radar Technology*, Telecommunications and Radio Engineering, V.55(2001), #12, pp.8-

[2] Lukin, K.A. *Noise Radar Technology: the Principles and Short Overview,* Applied Radio Electronics, V.4, #1, pp. 4-13, (2005).

[3] A.A. Mogyla, K.A.Lukin, Y.A.Shiyan, “Ambiguity Function of Noise Pulses Train and its Distortions in Noise Radar Receiver”, Proc. of IRS 2004, International Radar Symposium, 19-21 May 2004, Warszawa, Poland, 2004, pp. 37 – 42.

[4] Lukin, K. A., Mogyla, A. A., Palamarchuk, V. P., Vyplavin, P. L. Zemlyaniy, O. V., Shiyan, Y. A. and Zaets, M., ‘Ka-band Bistatic Ground-Based Noise Waveform SAR for Short-Range Applications,’ IET Proc. Radar Sonar & Navig., **2**, pp 233-243, August 2008.

[5] D. Tarchi, K.Lukin, J.Fortuny-Guasch, A. Mogyla, P.Vyplavin, A. Sieber, SAR imaging with noise radar, IEEE Transactions on Aerospace and Electronic Systems, vol. 46, no.3, July 2010.

[6] K.A. Lukin, “A Novel Approach to Scanning Antenna Design”, Proceedings 4th Int. Conf. on Antenna Theory and Techniques, Sevastopol, Vol. 11, pp. 290-293, 2003.

[7] K.A. Lukin, “Sliding Antennas for Noise Waveform SAR” // Applied Radio Electronics, 2005, Vol. 4, No. 1, pp. 103-106.

[8] K.A. Lukin, “Scanning Antennae with Beam Synthesis.” // Radioelectronics. 2010,vol.53, No. 4, pp. 58-64.

Manuscript received December, 12, 2012

Konstantin A. Lukin, for photograph and biography, see this issue, p. 24.

Andy Stove, for photograph and biography, see this issue, p. 121.

Krzysztof S. Kulpa (M’1991, SM’2010), Ph.D in electronics. Since 1990 he is Associate Professor at Institute of Electronic Systems (WUT). He is now the head of Digital Signal Processing Laboratory, and head of Radar Technology Research Group at WUT. Since 2011 he is the Scientific Director of Defense and Security Research Center of Warsaw University of Technology. His research interests involve radar signal and data processing including detection, tracking, PCL, SAR, ISAR and noise radars. He is a senior member of IEEE and a member of EUMA and AOC. He is the vice-chairman of the joint Polish chapter IEEE AESS/AP/MTT.

David Calugi Since 1986 works at Radar Department of Selex – ES (Ex SMA) – Florence, Italy. He participated in development the first Italian radar for air combat airplanes. Scientific interests are in avionic radars, noise radars, SAR imaging, tracking algorithms as TWS systems, applied Polarimetric radar to detection and classification of target. He is a member of IEEE and AI AA.

Palamarchuk Vladimir Petrovich, for photograph and biography, see this issue, p. 144.

Vyplavin Pavel Leonidovich, for photograph and biography, see this issue, p. 94.

УДК 621.37

Испытания наземного шумового РСА 8-мм диапазона в различных условиях / К.А. Лукин, А.Г. Стоув, К. Кульпа, Д. Калуджи, В.П. Паламарчук, П.Л. Выплавин // Прикладная радиоэлектроника: науч.-техн. журнал. – 2013. Том 12. № 1. – С. 145–151.

Интерес к шумовым радарам растет, поскольку они обеспечивают наилучшую электромагнитную совместимость, малую вероятность перехвата и использования сигналов и другие положительные свойства, в то время как прогресс в электронике делает их все более доступными. Одной из сфер применения шумовых сигналов являются радары с синтезированной апертурой (РСА). Для правильной работы РСА требуется высокая стабильность параметров радара, включая параметры зондирующего сигнала. Данная работа посвящена экспериментальному исследованию 8-мм наземного шумового РСА и оценке уровня шума, динамического диапазона, разрешения по дальности, остаточных флуктуаций и боковых лепестков. В работе мы кратко описываем устройство шумового наземного РСА и представляем результаты измерений.

Ключевые слова: шумовой радар, РСА, интерферометрия

Ил.14. Библиогр.: 8 назв.

УДК 621.37

Випробовування наземного шумового РСА 8-мм діапазону у різних умовах / К.О. Лукін, А.Г. Стоув, К. Кульпа, Д. Калуджі, В.П. Паламарчук, П.Л. Виплавін // Прикладна радіоелектроніка: наук.-техн. журнал. – 2013. Том 12. № 1. – С. 145–151.

Інтерес до шумових радарам росте, оскільки вони забезпечують найкращу електромагнітну сумісність, малу ймовірність перехоплення і використання сигналів та інші позитивні властивості, в той час як прогрес в електроніці робить їх все більш доступними. Однією зі областей застосування шумових сигналів є радари з синтезованою апертурою (РСА). Для правильної роботи РСА потрібна висока стабільність параметрів радара, включаючи параметри сигналу. Дана робота присвячена експериментальному дослідженню 8-мм наземного шумового РСА та оцінці рівня шуму, динамічного діапазону, розрізнення по дальності, залишкових флуктуацій і бічних пелюсток. У роботі ми коротко описуємо пристрій шумового наземного РСА і представляємо результати вимірювань.

Ключові слова: шумовий радар, РСА, інтерферометрія.

Іл. 14. Бібліогр.: 8 найм.